

Superconductivity in U-T Alloys (T = Mo, Pt, Nb, Zr) Stabilized in the Cubic γ -U Structure

S. SOWA^a, N.-T.H. KIM-NGAN^{a,*}, M. KRUPSKA^a, M. PAUKOV^b, I. TKACH^b AND L. HAVELA^b

^aInstitute of Physics, Pedagogical University, Podchorążych 2, 30-084 Kraków, Poland

^bFaculty of Mathematics and Physics, Charles University, Ke Karlovu 5, 12116 Prague, Czech Republic

Using ultrafast cooling (with the cooling rate up to 10^6 K/s) helps to minimize the T-alloying concentration (T = Mo, Pt, Pd, Nb, Zr) necessary to retain the γ -U phase down to low temperatures. All investigated splat-cooled U-T alloys become superconducting with T_c in the range of 0.61–2.11 K. The bulk character of superconductivity can be concluded for some of the splats when comparing the specific-heat anomaly at T_c with the BCS theory prediction.

DOI: [10.12693/APhysPolA.130.521](https://doi.org/10.12693/APhysPolA.130.521)

PACS/topics: 81.05.Bx, 74.70.Ad, 72.15.Cz

1. Introduction

Low-temperature physical properties of uranium has been investigated thoroughly for the orthorhombic α -U phase (space group $Cmcm$) [1], since only this phase is stable at and below room temperature. The superconductivity of (natural) uranium was first discovered in 1942 at 1.3 K, while more recent data reported $T_c = 0.78$ K [2, 3]. However, no signature of superconductivity was found down to 0.02 K at ambient pressure in good-quality single crystals of uranium, although the charge-density-wave (CDW) states [3] were found to be developed fully at low temperatures in those crystalline uranium specimens [4]. The γ -U phase with a body-centered-cubic structure (space group $Im\bar{3}m$) is stable at high temperatures between 1049 ± 2 – 1408 K [1]. It can be retained to the room temperature by alloying with Zr, Nb, Mo, Pd, Pt, etc. [5]. For instance the single-phase γ -U alloy has been reported for the U-8 wt% Mo (U-16.5 at.% Mo) under normal furnace cooling conditions [6].

The $5f$ electronic states in many uranium-based compounds are generally close to the verge of localization, which brings up fascinating many-body physics from the fundamental research viewpoint. In this respect it is necessary to determine the basic thermodynamic properties of the less-known γ -U phase alloys, since they exhibit a superconducting ground state around $T = 2$ K. There exist only old reports from 1960s on the superconductivity of the γ -U phase around 2 K in water-quenched U-Mo and U-Nb alloys [7]. There is a lack of detailed and recent data on fundamental low-temperature properties of the γ -U alloys.

Recently, using ultrafast cooling (from the melt to room temperature), we can retain the cubic γ -U phase with a lower concentration of alloying elements down to room temperature. Moreover, those γ -U alloys are

very stable when exposed to air (i.e., no ageing effect or phase transformation/decomposition). Thus we can proceed with characterization of low-temperature properties of those γ -U phase alloys. Starting with Mo alloying, we succeeded to suppress any α -U phase for about 11 at.% Mo [8, 9]. In the present work we present our work in stabilization of the γ -U phase by a combination of ultrafast cooling and other T alloying (T = Pt, Pd, Nb, Zr). We focus on investigations of the superconducting phase transition in those alloys. The results are compared with those obtained earlier for U-Mo splats.

2. Experimental

U-T alloys (T = Mo, Pt, Pd, Nb, Zr) were prepared using natural U (2N8 purity or better) and T element (3N8 or better) by arc-melting on a copper plate in argon atmosphere. The splat-cooled sample was prepared from the alloy-ingot by splat-cooling technique (using the HV splat cooler from Vakuu Praha) and had a shape of irregular disc with a diameter of approximately 20 mm and a thickness of 100–200 μm . In our equipment, the molten metal is dropped between two colliding massive copper pistons, yielding a cooling rate better than 10^6 K/s [8].

The crystal structure of splat-cooled alloys (splats) was investigated by X-ray diffraction (XRD) using the Bruker D8 Advance diffractometer with Cu K_α radiation. The resistivity and specific heat measurements were carried out in the temperature range 0.3–300 K by means of standard techniques, such as closed cycle refrigerator system (CCR), Quantum Design Physical Properties Measurement System (PPMS), described earlier [8–10].

Additional phase purity analysis was performed in the scanning electron microscope (SEM) equipped with a energy dispersive X-ray (EDX) analyzer. The splats show a homogeneous distribution of the alloying elements, the concentration of which corresponds to the nominal one. Electron backscattering diffraction (EBSD) analysis has been employed to study the microstructure and texture of selected U-T splats. (For more information see e.g.

*corresponding author; e-mail: tarnawsk@up.krakow.pl

Ref. [8].) The EBSD map for example for U-15 at.% Mo splat revealed only γ -U phase with no evidence for α or α -U related phases, confirming the XRD data.

3. Results and discussions

We have started with U-Mo splats and thus more splats with Mo concentration of 0 (pure U splat), 1, 2, 4, 6, 10, 11, 12, 13, 15, 17 at.%, have been prepared and investigated so that we could determine precisely the minimal Mo concentration necessary for obtaining the pure cubic γ -U phase. Details of our investigations of crystal structure and phase stability have been reported elsewhere [8–10]. The most important outcome is that the ideal bcc A2-type structure was obtained in U-15 at.% Mo alloy revealed by very sharp γ -reflections (see e.g. the γ -(110) reflection shown in Fig. 1 in Ref. [9]). The effect of splat cooling can be seen also in a better capability in retaining the bcc-type of structure for lower (by several at.%) Mo concentrations. On the other hand, the splat cooling does not affect the crystallinity: the materials do not turn amorphous.

We have extended our studies to the splat-cooled U-based alloys with other T metals. We focus our attention on obtaining the splats having γ -U phase. Thus we produced only splats with chosen T contents. Besides, there is a similarity between Pt- and Pd-doped alloys, and thus we concentrate more on Pt-doped alloys. In general, the XRD data show that increase of the T concentration leads to a suppression of the low-index α -U reflections, vanishing of the high-index α -U reflections and a development of γ -U reflections. In most cases, the γ -U phase becomes very dominant by doping with 15 at.% T content (T = Pt, Pd, Nb). The situation is different for U-Zr system. Namely, a much higher Zr concentration is needed to suppress the α -U phase. Although a large reduction of α -U with increasing Zr concentration is clearly seen by the decrease of the α (110) and α (111) peaks (the most dominant α -U reflections), but they still persist for U-15 at.% Zr. They become very broad for U-20 at.% Zr splats and vanish only in U-30 at.% Zr splat. Moreover, most of γ -reflections including the main peak γ (111) at 35.9° in this splat are very broad. We notice here that the existing report [11] indicated that the single-phase γ -alloys were obtained for Zr concentrations between 25 at.% and 80 at.%.

For a brief illustration of the crystal structure investigations of splat-cooled U-T splats, we show in Fig. 1 the most intense γ (110) reflection in XRD patterns at around $2\theta = 37^\circ$, in a comparison with that of U-15 at.% Mo consisting of a pure single γ -U phase. Our results indicate that the bcc structure could be stabilized in U-15 at.% Pt splat. However, the γ -peak in this splat is quite broad, similar to those of U-13 at.% Mo splat. Moreover, a very small trace of α -U phase is still present. It is interesting to compare our findings with respective binary phase diagrams. We notice here that the maximum solubility in γ -U of Pt or Pd has been reported not exceeding

5 at.% [5, 12]. Our results indicate that using the splat cooling we not only retain the bcc phase to low temperatures but also extend its occurrence for much higher concentrations of alloying Pt metals (15 at.%). Alloying with 15 at.% Nb seems to stabilize the γ^0 -U phase revealed by γ -doublets. However, a much larger broadening of γ^0 -peaks was observed for U-15 at.% Nb splat, in a comparison with those e.g. for U-12 at.% Mo splat. We also add to the figure the data for U-30 at.% Zr exhibiting the γ -U phase. The γ (110) peak is relocated to lower angles reflecting a lattice expansion.

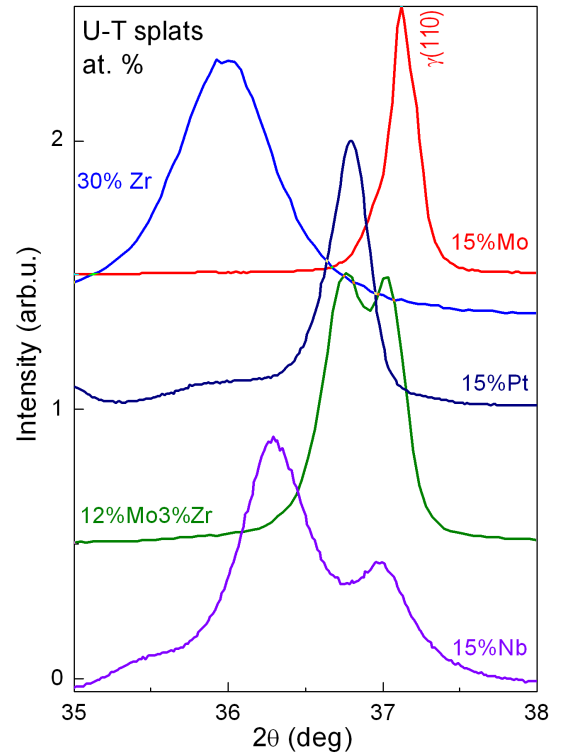


Fig. 1. Illustration of the most intense reflection in (normalized) XRD patterns of splat-cooled U-T splats with 15 at.% T (T = Mo, (Mo + Zr), Pt, Nb) and 30 at.% Zr alloying. Sharp γ -U peaks with no trace of any α -U peaks revealing the ideal cubic structure were observed only for U-15 at.% Mo.

We have also investigated the crystal structure of U-12 at.% Mo-3 at.% Zr splat, i.e. with combined 12 at.% Mo plus 3 at.% Zr alloying (U-15 at.%(Mo + Zr)). Doublets were observed for all γ -peaks, indicating that it leads to the γ^0 -U structure. The peaks are quite narrow, similar to those of U-12 at.% Mo [8]. Besides, the most intense doublet assigned to γ^0 (101) and γ^0 (110) reflections (at respectively 36.8° and 37.0°) of U-15 at.%(Mo + Zr) is more symmetric and with roughly equal intensity. In other words, replacing 3 at.% Mo by 3 at.% Zr implies a small tetragonal distortion and the pure bcc structure (γ -U phase (in U-15 at.% Mo) has changed into a body centered tetragonal structure (γ^0 -U phase). The lattice param-

eters estimated are: $a(\text{U-15 at.}\% \text{ Pt}) = 3.45 \text{ \AA}$, $a(\text{U-15 at.}\% \text{ Nb}) = 3.43 \text{ \AA}$ (and $c(\text{U-15 at.}\% \text{ Nb}) = 3.57 \text{ \AA}$), $a(\text{U-15 at.}\% (\text{Mo} + \text{Zr})) = 3.43 \text{ \AA}$ (and $c(\text{U-15 at.}\% (\text{Mo} + \text{Zr})) = 3.48 \text{ \AA}$). Indeed, the $\gamma(110)$ reflection in U-15 at. % Nb, U-15 at. % Pt and U-15 at. % (Mo + Zr) locates at around 37.0° , i.e. at the similar angle for that of the pure cubic U-15 at. % Mo alloy ($a(\text{U-15 at.}\% \text{ Mo}) = 3.44 \text{ \AA}$), indicating that the a -parameter in these two alloys is similar to that of the bcc structure of U-15 at. % Mo. Doping with 15 at. % Zr certainly leads to a large expansion of the lattice ($a(\text{U-15 at.}\% \text{ Zr}) = 3.54 \text{ \AA}$), the relative increase of the lattice (Δa) is estimated to be about 3%.

The temperature dependence of resistivity in the range 0.3–300 K thoroughly investigated for U-Mo alloys with different Mo concentrations ranging from 0 to 15 at. % was reported earlier [8–10]. For a comparison with other systems, we show in Fig. 2 the two limits which reveals a striking difference: the pure-U splat consisting of pure α -U phase and the U-15 at. % Mo splat consisting of the γ -U phase. The pure-U splat exhibits a quadratic temperature dependence below 50 K and a nearly linear dependence up to 300 K. For U-15 at. % Mo, the resistivity increases with decreasing temperature from 300 K down to temperature just above the superconducting transition temperature, i.e. revealing a negative temperature coefficient/slope ($d\rho/dT < 0$). We remind here that the negative value of $d\rho/dT$ was exhibited for all U-Mo alloys with γ -U phase (with ≥ 11 at. % Mo doping), while those consisting of both α - and γ -U phase (with ≤ 10 at. % Mo doping) still have the positive one [8]. The temperature dependence of the resistivity of U-15 at. % T splats ($T = \text{Nb, Pt}$) in the temperature range 4–300 K is shown in the same figure (Fig. 2), as the normalized $\rho/\rho_{300\text{ K}}(T)$ curves. The residual resistivity ρ_0 ($\rho_{4\text{ K}}$) and the resistivity at room temperature ($\rho_{300\text{ K}}$) of U-15 at. % Nb spat are similar with those of U-15 at. % Mo ($\rho_{300\text{ K}}(\text{U-15 at.}\% \text{ Nb}) = 83 \mu\Omega\text{cm}$, $\rho_{4\text{ K}}(\text{U-15 at.}\% \text{ Nb}) = 86 \mu\Omega\text{cm}$, $\rho_{300\text{ K}}(\text{U-15 at.}\% \text{ Mo}) = 89 \mu\Omega\text{cm}$, $\rho_{4\text{ K}}(\text{U-15 at.}\% \text{ Mo}) = 95 \mu\Omega\text{cm}$), while those for U-15 at. % Pt splats are twice higher ($\rho_{300\text{ K}}(\text{U-15 at.}\% \text{ Pt}) = 164 \mu\Omega\text{cm}$, $\rho_{4\text{ K}}(\text{U-15 at.}\% \text{ Pt}) = 166 \mu\Omega\text{cm}$). However, the relative change of the resistivity in those splats (with 15 at. % T doping ($T = \text{Mo, Pt, Nb}$)) is very similar, exhibiting a negative temperature coefficient ($d\rho/dT < 0$). We suggest that for U-based splat-cooled alloys, a large disorder effect plays an important role for the splat-cooled alloys, similar to a strong disorder observed e.g. in some amorphous systems and the Heusler alloys [13]. In our case, there is certainly still some extra contribution to the disorder produced by ultrafast cooling. For U-30 at. % Zr splat revealing the γ -U phase, we found a very small (close to zero) but still positive slope of the temperature dependence, i.e. the negative slope does not develop yet, despite of the fact that the $\rho_{4\text{ K}}$ and $\rho_{300\text{ K}}$ values are in the same range with those

of U-15 at. % Mo ($\rho_{300\text{ K}}(\text{U-15 at.}\% \text{ Zr}) = 75 \mu\Omega\text{cm}$, $\rho_{4\text{ K}}(\text{U-15 at.}\% \text{ Zr}) = 73 \mu\Omega\text{cm}$). We notice here that a negative coefficient ($d\rho/dT < 0$) was reported for U-Zr system, but with 70 at. % Zr [14]. Thus we can expect that a negative slope can be observed for U-Zr splats, but certainly for higher Zr concentrations (> 30 at. % Zr).

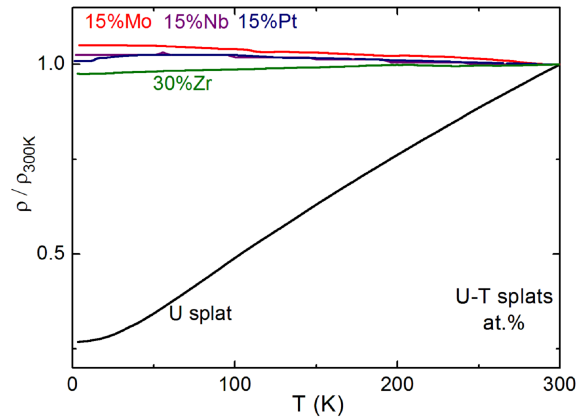


Fig. 2. Temperature dependence of the normalized electrical resistivity in the normal state. The alloys with γ -U phase (15 at. % T doping ($T = \text{Mo, Pt, Nb}$)) have a negative value of $d\rho/dT$, except of U-30 at. % Zr has a positive one.

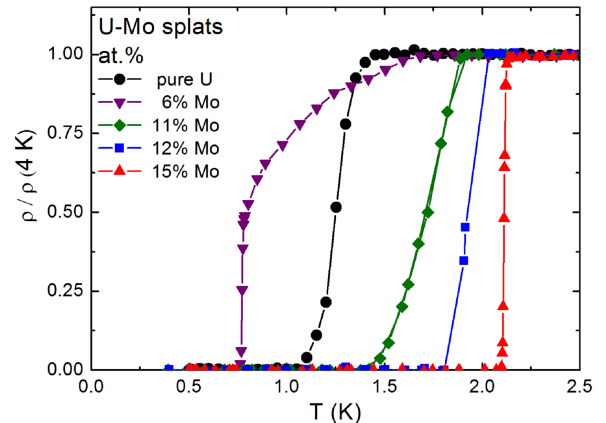


Fig. 3. Superconducting phase transition revealed by the resistivity drop(s) in zero field in U-Mo splats. The pure single γ -U phase U-15 at. % Mo alloy has a highest critical temperature ($T_c = 2.11 \text{ K}$) and narrowest transition width ($\Delta T_p = 0.02 \text{ K}$).

All investigated U-T splats become superconducting at low temperatures. For a short summary of U-Mo system, we present in one figure (Fig. 3) the superconducting transitions observed in all investigated splats in zero magnetic field. The transition is manifested by a single abrupt drop at T_c observed for pure U splat (α -U phase) and all γ -U splats (11–15 at. % Mo). The sharpest transition with a transition width of $\Delta T_p = 0.02 \text{ K}$ and a highest critical temperature $T_c = 2.11 \text{ K}$ was obtained for

U-15 at.% Mo, i.e. the only splat sample with the pure single γ -U phase with ideal A2 bcc structure [15]. We pay particularly attention to the superconducting transition in the U-6 at.% Mo splat, i.e. with the intermediate range of Mo doping consisting of both α - and γ -U phase. The resistivity starts to decrease below 1.6 K, which has to be interpreted as emergence of a small amount of superconducting phase. This decrease ends in an abrupt drop into the zero resistance state at $T_c = 0.78$ K. It shows that there are two different superconducting phases in this splat, each exhibiting its own superconductivity. The lower T_c is attributed to the γ -U phase, as revealed by a sizeable anomaly in the specific heat [10].

The low-temperature $\rho(T)$ dependence of other U-T splats having γ -U phase measured in zero field is shown in Fig. 4. U-15 at.% Nb has revealed as a single drop at $T_c = 1.90$ K with a transition width $\Delta T_\rho = 0.15$ K. Except of a small difference in the T_c values, the resistivity drop in U-15 at.% Nb is very similar to that of U-Mo splats consisting of γ^0 -U structure (with 11–12 at.% Mo). For U-15 at.% Pt, a sharp drop was observed at $T_c = 0.61$ K with a very small transition width $\Delta T_\rho = 0.04$ K. Despite of a similarity in the crystal structure (γ -U) and lattice parameter between U-15 at.% Mo and U-15 at.% Pt (resulted from alloying with elements with a similar atomic radii), U-15 at.% Pt becomes superconducting at a much lower temperature. Besides, an extra small drop was observed at $T_c(h) = 0.95$ K with a transition width $\Delta T_\rho = 0.08$ K. U-30 at.% Zr exhibits a superconducting transition revealed by a single drop at $T_c = 0.81$ K with a transition width $\Delta T_\rho = 0.08$ K.

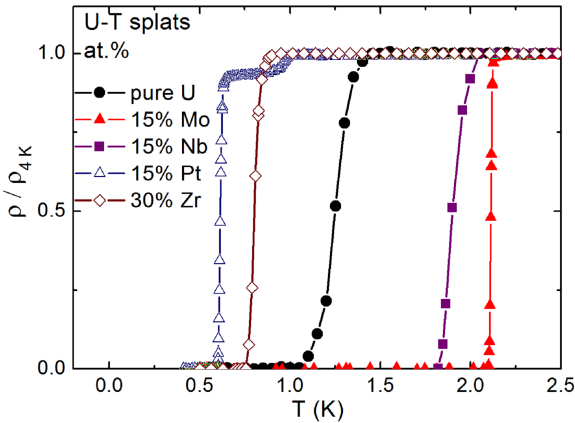


Fig. 4. The resistivity drop in zero field related to the superconducting phase transition for investigated U-T splat alloys having γ -U phase. The data for pure-U splat were also shown for a comparison.

More detailed investigations of superconducting phase transition in U-15 at.% Pt are in progress in order to understand the two transitions below T_c and $T_c(h)$. We notice here that, even if for the U-5 at.% Pt splat consisting of a mixed α -U and γ -U phase, the superconducting phase transition is revealed by only a single

drop in the resistivity [10]. The results support that the existence of two critical temperatures T_c and $T_c(h)$ in U-15 at.% Pt splat is certainly not contributed to the existence of two phases with different crystal structures (e.g. α -U and γ -U phase), rather it is an evidence of the existence of two different superconducting phases. The situation is quite similar to that observed recently in the skutterudite-related $\text{La}_3\text{Rh}_4\text{Sn}_{13}$ [16] and $\text{La}_3\text{Ru}_4\text{Sn}_{13}$ [17] superconductors. Namely, the high temperature inhomogeneous superconducting state below T_c^* and the second (bulk) superconducting phase below T_c — the bulk phase ($T_c < T_c^*$). For convenience in our paper we use $T_c(h)$ instead of T_c^* . The higher temperature superconducting phase between T_c and $T_c(h)$ is interpreted in the context of electronic disorder over length scales similar to the coherence length often observed in the high- T_c superconductors. Besides, the local nanoscaled disorder is considered to be responsible for the increase in T_c in inhomogeneous regions in the sample. We notice here that the presence of inhomogeneities of superconducting characteristics has been reported for many novel superconducting materials, not only in a polycrystal but also in a single crystal. Unlike e.g. $\text{La}_3\text{Rh}_4\text{Sn}_{13}$ compound which is a typical BCS superconductor with a sizable λ -type peak observed in the specific-heat at T_c (and a change of the slope of $C(T)$ at $T_c(h)$ at which a sharp drop was revealed in the resistivity), no sizable specific-heat peak was observed for U-15 at.% Pt splat at around T_c or $T_c(h)$.

Applying external magnetic fields, the superconducting transitions shift towards lower temperatures, as expected. The estimated critical magnetic fields at zero temperature ($\mu_0 H_c$) are in the range of 2–7 T, and the critical slopes at T_c of the H_{c2} vs. T curves ($-\mu_0(dH_{c2}/dT)_{T_c}$) are in the range of 2–4 T/K. These values are close to that found for the strongly interacting Fermi liquid superconductor U_6Fe ($-\mu_0(dH_{c2}/dT)_{T_c} = 3.42$ T/K) [16] as well as within the limit for the extreme high-field A15 and Chevrel-phase superconductors ($2T/K \leq (-\mu_0(dH_{c2}/dT)_{T_c} \leq 8$ T/K). One difference is that for those splat-cooled γ -U alloys, the T_c values are lower than 2.2 K, while Chevrel-phase superconductors have much higher T_c (> 10 K).

The temperature dependence of specific heat, $C_p(T)$, has been studied for selected splats over the whole temperature range 0.3–300 K, for characterizing the superconducting behavior as well as the electronic and phonon contribution. The Sommerfeld coefficient of electronic specific heat (γ_e) and the Debye temperature (Θ_D) can be estimated from the C_p/T vs. T^2 plot in the normal state. ($C_p/T = \gamma_e + \beta T^2$; $\beta = 234N_A k_B / (\Theta_D)^3$ for C_p [J/(mol K)]). A clear evidence of an increase of density of states at the Fermi level for γ -U is observed, as shown by an enhancement of the γ_e value by Pt doping ($\gamma_e = 19.5$ mJ/(K² mol) (≈ 23 mJ/(K² mol U) for U-15 at.% Pt, in a comparison with that for pure U $\gamma_e = 11$ mJ/(K² mol U)). It is ascribed to e.g. the increasing atomic volume and higher U-U spacing. The

enhancement of the γ_e value and the softening of the lattice (revealed by reduction of the Debye temperature) is found to be smaller for Nb and Zr alloying. The Debye temperature was estimated to be $\Theta_D \approx 145$ K for U-15 at.% Pt.

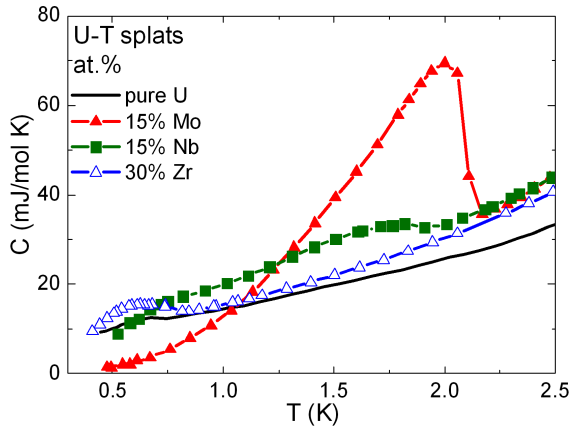


Fig. 5. Specific-heat anomalies related to the superconducting phase transition for selected U-T splats. A typical BCS superconductivity was observed only for U-15 at.% Mo alloy.

The temperature dependence of the specific heat has been performed down to 0.3 K for selected splat-cooled U-T alloys. We estimated the height of the experimentally observed specific-heat jump (ΔC). It was then compared to the estimated BCS value ($\Delta C = 1.43\gamma_e T_c$) by using the γ_e and T_c values determined from our experiments [15]. In Fig. 5, we shown again the C - T curves in zero field for the two limits: the pure-U and U-15 at.% Mo splat. Only a very small feature related to the superconducting transition was revealed at 0.65 K in the specific heat for the pure-U splat. The results suggest that only a small fraction of the sample is really superconducting. For U-15 at.% Mo splat, a pronounced λ -type specific-heat anomaly was observed at T_c determined from resistivity jump. The height of the experimentally observed specific-heat jump (ΔC) is in a good agreement with that estimated from BCS theory (see e.g. Fig. 5 in Ref. [15]). Such a BCS-type superconductivity in U-15 at.% Mo revealed that it might be in analogy with that of U_6Fe [18]. With lower Mo contents, the observed specific-heat jumps are much lower than those estimated BCS values [10]. The specific-heat data for other selected γ -U splats around the superconducting phase transition are also presented in Fig. 5. Only a weak and broad bump was observed in $C(T)$ curve of U-15 at.% Nb. In fact, the crystal structure, the resistivity jump and T_c value of U-15 at.% Nb splat are similar to that of U-12 at.% Mo splat. However, while a still quite large peak was observed for U-12 at.% Mo, the superconducting transition in U-15 at.% Nb revealed by only a much broader bump and with a much smaller height in $C(T)$ curve. The specific heat peak related to the superconducting transition

in U-30 at.% Zr splat is visible and at T_c determined from the resistivity jump, revealing that the superconductivity in the U-30 at.% Zr is a real bulk effect.

We employ the McMillan expression [19] to evaluate the electron-phonon coupling parameter λ from the relation between λ and T_c and the Debye temperature Θ_D and the Coulomb repulsion m^* (the value of m^* was chosen to be 0.1 for s and p band superconductors). This yields $\lambda = 0.41$ and 0.45 , respectively for T_c and $T_c(h)$ for U-15 at.% Pt alloy. The results indicate that both superconducting states could not be attributed to the strong-coupling superconductivity.

4. Summary

The γ -U phase were retained in the U-T alloys by a combination of ultrafast cooling and doping with 15 at.% T content ($T = \text{Mo, Pt, Nb}$) and/or 30 at.% Zr content. However, an ideal cubic $A2$ structure was found only for U-15 at.% Mo splat. Our results confirm that Mo is the best alloying element for stabilization of the γ -U structure. Moreover, by using ultrafast cooling we are able to reduce the necessary concentration of the T elements for obtaining γ -U phase in the normal state, without any additional sample-treatment.

All the U-T splats become superconducting with T_c in the range of 0.61–2.11 K. The prediction of BCS superconductivity for the specific-heat jump at T_c was found to be fulfilled only in the U-15 at.% Mo splat among all investigated splats.

In the context of the stability of the bcc U-T alloys it is interesting to mention their improved resistance to hydrogen absorption. While α -U easily absorbs hydrogen even at room temperature and at a few mbar of H_2 forming UH_3 (which is a pyrophoric substance), the cubic γ -U phase does not absorb hydrogen below 2.5 bar. Preliminary data on other γ -U splats (U-15 at.% Pt and U-15 at.% Nb) indicate a hydrogen resistance as well. We have demonstrated that elevated pressures $p(\text{H}_2) > 2.5$ bar are needed to achieve hydrides of equivalent stoichiometry for U-Mo [20] and U-Zr alloys [21]. The lattice expansion due to hydrogen absorption leads to the disappearance of superconductivity and the formation of U magnetic moment and the antiferromagnetic order in these hydrides.

Acknowledgments

This work was supported by the Czech Science Foundation under the grant No. 15-01100S. Experiments were partly performed at MLTL (<http://mltl.eu/>) supported within the program of Czech Research Infrastructures (project No. LM2011025). The participation of Kraków group was supported by the Czech-Polish cooperation in the scope of Czech-Polish project 7AMB14PL036 (9004/R14/R15). N-T.H.K.-N. acknowledges the European Regional Development Fund under the Infrastructure and Environment Programme.

References

- [1] I. Grenthe, J. Drozdzyński, T. Fujino, E.C. Buck, T.E. Albrecht-Schmitt, S.F. Wolf, in: *The Chemistry of the Actinide and Transactinide Elements*, Eds. L.R. Morss, N. Edelstein, J. Fuger, J.J. Katz, Springer, 2006, Ch. 5.
- [2] G.H. Lander, E.S. Fisher, S.D. Bader, *Adv. Phys.* **43**, 1 (1994).
- [3] J.C. Lashley, B.E. Lang, J. Boerio-Goates, B.F. Woodfield, G.M. Schmiedeshoff, E.C. Gay, C.C. McPheeters, D.J. Thoma, W.L. Hulst, J.C. Cooley, R.J. Hanrahan, J.L. Smith, *Phys. Rev. B* **63**, 224510 (2001).
- [4] D. Graf, R. Stillwell, T.P. Murphy, J.-H. Park, M. Kano, E.C. Palm, P. Schlottmann, J. Bourg, K.N. Collar, J. Cooley, J. Lashley, J. Willit, S.W. Tozer, *Phys. Rev. B* **80**, 241101(R) (2009).
- [5] G.L. Hofman, M.K. Meyer, A.E. Ray, in: *Proc. Int. Reduced Enrichment for Research and Test Reactors Conf.*, Sao Paulo 1998.
- [6] V.P. Sinha, P.V. Hegde, G.J. Prasad, G.K. Dey, H.S. Kamath, *J. Alloys Comp.* **506**, 253 (2010) and references therein.
- [7] B.S. Chandrasekhar, J.K. Hulm, *J. Phys. Chem. Solids* **7**, 259 (1958).
- [8] I. Tkach, N.-T.H. Kim-Ngan, S. Mašková, M. Dzevenko, L. Havela, A. Warren, C. Stitt, T. Scott, *J. Alloys Comp.* **534**, 101 (2012).
- [9] N.-T.H. Kim-Ngan, I. Tkach, S. Mašková, A.P. Goncalves, L. Havela, *J. Alloys Comp.* **580**, 223 (2013).
- [10] N.-T.H. Kim-Ngan, M. Paukov, S. Sowa, M. Krupská, I. Tkach, L. Havela, *J. Alloys Comp.* **645**, 158 (2015).
- [11] J.G. Huber, P.H. Ansari, *Physica B* **135**, 441 (1985).
- [12] B.A.S. Ross, D.E. Peterson, *Bull. Alloy Phase Diagr.* **11**, 240 (1990).
- [13] A. Ślebarski, J. Goraus, J. Deniszczczyk, L. Skoczen, *J. Phys. Condens. Matter* **18**, 10319 (2006).
- [14] R.D. Barnard, *Proc. Phys. Soc.* **78**, 722 (1961).
- [15] I. Tkach, N.-T.H. Kim-Ngan, A. Warren, T. Scott, A.P. Goncalves, L. Havela, *Physica C* **498**, 14 (2014).
- [16] A. Ślebarski, M. Fijałkowski, M.M. Maška, M. Mierzejewski, B.D. White, M.B. Maple, *Phys. Rev. B* **89**, 125111 (2014).
- [17] A. Ślebarski, M.M. Maška, M. Fijałkowski, C.A. McElroy, M.B. Maple, *J. Alloys Comp.* **646**, 866 (2015).
- [18] L.E. DeLong, J.G. Huber, K.N. Yang, M.B. Maple, *Phys. Rev. Lett.* **51**, 312 (1983).
- [19] W.L. McMillan, *Phys. Rev.* **167**, 331 (1968).
- [20] I. Tkach, S. Maskova, Z. Matej, N.-T.H. Kim-Ngan, A.V. Andreev, L. Havela, *Phys. Rev. B* **88**, 060407(R) (2013).
- [21] I. Tkach, M. Paukov, D. Drozdenko, M. Cieslar, B. Vondrackova, Z. Matej, D. Kriegner, A.V. Andreev, N.-T.H. Kim-Ngan, I. Turek, M. Divis, L. Havela, *Phys. Rev. B* **91**, 115116 (2015).